INSTITUTE OF PHYSICS PUBLISHING PHYSICS IN MEDICINE AND BIOLOGY

Phys. Med. Biol. **51** (2006) N9–N16 doi:10.1088/0031-9155/51/1/N02

NOTE

Estimating perfusion using microCT to locate microspheres

M Marxen[1,2], C Paget[2], L X Yu[3] and R M Henkelman[1,2,3]

[1] Department of Medical Biophysics, University of Toronto, Toronto, Canada
[2] Sunnybrook and Women's College Health Sciences Centre, University of Toronto, Toronto, Canada
[3] Hospital for Sick Children—Mouse Imaging Centre (MICe), 555 University Ave, Toronto, ON, M5G 1X8, Canada

E-mail: mhenkel@phenogenomics.ca

Received 29 June 2005, in final form 3 October 2005
Published 14 December 2005
Online at stacks.iop.org/PMB/51/N9

Abstract

The injection of microspheres into the blood stream has been a common method to measure the spatial distribution of blood flow (perfusion). A technique to conduct this kind of measurement in small animal organs is presented using silver-coated microspheres with a diameter of 16 μm and high-resolution computed tomography (microCT) to detect individual microspheres. Phantom experiments demonstrate the detectability of individual spheres. The distribution of microspheres within a rat heart is given as an example. Using non-destructive, three-dimensional imaging for microsphere detection avoids the cumbersome dissection of the organ into samples or slices and their subsequent registration. The detection of individual spheres allows high-resolution measurements of perfusion and arbitrary definition of regions of interest. These, in turn, allow for accurate statistical analysis of perfusion such as relative dispersion curves.

Introduction

Knowledge of perfusion, defined as the volume of blood delivered to a certain mass of tissue per unit time, is important in the study of healthy and pathological blood flow physiology. Determining microsphere deposition density has been one of the most common and well-established techniques to measure local perfusion for decades. The technique has been described in detail by Heymann *et al* (1977) and has been reviewed by Prinzen and Bassingthwaighte (2000). The diameter of the injected microspheres is approximately 15 μm and is chosen such that the spheres lodge in small arterioles close to the perfusion site of interest and do not cross the capillary bed. Assuming ideal mixing and flow tracing of the

microspheres within the blood stream, the local density of trapped microspheres is regarded as proportional to local perfusion.

A variety of microsphere types and analysis techniques have been employed to obtain local microsphere densities. Radioactive, coloured and fluorescent microspheres have been used as probes and analysed using gamma counters (Heymann *et al* 1977), optical spectrometers (Kawallik *et al* 1991, Wieland *et al* 1993) and two-dimensional optical imaging (Luchtel *et al* 1998). All of these techniques require dissection of the organ of interest into tissue pieces or slices. This article will demonstrate the feasibility of using silver-coated microspheres and three-dimensional, high-resolution computed tomography (microCT) to obtain the locations of individual microspheres in complete small animal organs in a convenient and non-destructive manner. CT provides discrete counting of individual microspheres along with simultaneous mapping of their individual locations in three dimensions.

Material and methods

Based on theoretical calculations of mass density and x-ray opacity, microspheres were custom-made by Microparticles GmbH, Berlin, Germany. Polystyrene beads with a diameter of 16 μm were coated with multiple layers of silver and gold. Samples were provided with different amounts of coating. The product codes AgVIII—L1080 and Ag/AuVIII—L1080 were found to provide the best compromise between mass density and x-ray absorption. The mass density of the AgVIII particles was estimated to be 2.0 ± 0.3 g cm^{-3} based on sedimentation velocity measurements by Microparticle GmbH. The particle diameter was confirmed to be 17 ± 1 μm using scanning electron microscopy (see figure 1).

Three-dimensional images were acquired using an MS90 eXplore Locus SP microCT scanner (General Electric Medical Systems, London, Ontario). The performance of this cone-beam CT scanner with rotating sample has been described in detail by Marxen *et al* (2004). Briefly, it is a rotate specimen scanner with a micro focus x-ray source and a 2000 pixel $\times$ 2000 pixel CCD detector. Three-dimensional images with isotropic voxel are reconstructed using the standard Feldkamp algorithm (Feldkamp *et al* 1984). Twelve hour scans with a detector pixel size in the object plane of 17 μm were performed at 80 kVp tube voltage and an exposure of 2592 mA s. The size of the reconstructed cubic volume elements (voxels) was also 17 μm.

Following several preliminary attempts, a phantom was constructed to prove the detectability of individual spheres. A small amount of particle powder was mixed into epoxy glue. A drop of the mixture was placed onto a 1.5 mm thick acrylic slide and pressed into a thin film between the slide and a thin (0.3 mm) sheet of plastic. Crosses of 25 μm copper wire had also been mounted onto the acrylic slide to provide a spatial reference. Optical micrographs of this planar arrangement of microspheres were taken before mounting the whole slide in a cylindrical sample vial (28 mm diameter) using 10% gelatin. CT images of the vial were then acquired with the slide being parallel to the axis of rotation of the CT. CT images were smoothened with a $3 \times 3 \times 3$ Gaussian kernel. Voxels above a threshold value of 150 HU in intensity are considered particles. This threshold was varied to determine the optimal setting as discussed in the results section. The number of particles within one connected set of voxels is assumed to be equal to the number of intensity maxima within the set. True positive fraction and false positive fraction are calculated using the optical images as truth.

As an application example, rat heart data from one of our experimental studies is presented. A Wistar rat was anaesthetized using ketamine/xylazine (75/10 mg kg^{-1} i.m.) and maintained using halothene inhalant. The heart was exposed through a midsternal incision, and about 4 ml of AgAuVIII particles (approximately 10^7 particles) suspended in Ringer's solution were

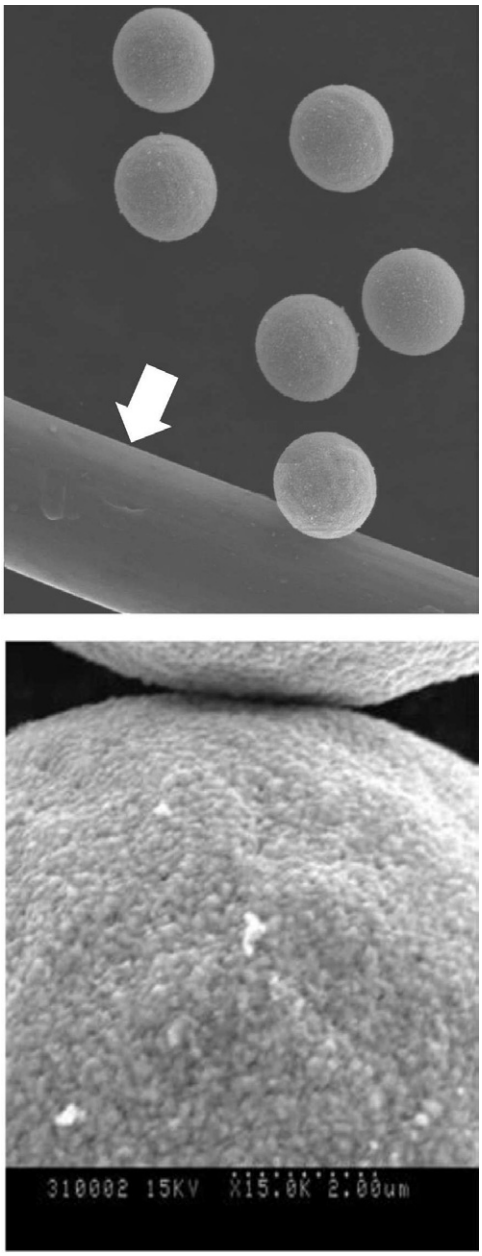

Figure 1. Scanning electron micrographs of silver-coated microspheres with a diameter of 17 μm. As a scale reference, there is a 25 μm copper wire in the upper image (arrow).

injected into the left atrium for about 10 s. After about 2 min of continued heart beating, the vascular system was flushed with Ringer's solution, the heart was excised and fixed in formalin. After about 48 h, the heart was mounted in the same type of sample vial as the phantom slides using agar. The animal procedures were approved by the Animal Care Committee of Sunnybrook and Women's College Health Sciences Centre. CT scanning was performed using the same parameters as in the phantom study.

Following the statistical analysis method introduced by Bassingthwaighte *et al* (1989), relative dispersion of perfusion (RD) within the myocardium was calculated as a measure of perfusion heterogeneity for different voxel volumes V:

$$\mathrm{RD}(V) = \sqrt{\frac{1}{P_{\mathrm{tot}}^2}\sum_i \frac{V_i}{V_{\mathrm{tot}}}(P_i - P_{\mathrm{tot}})^2 - \frac{1}{\bar{X}}},$$

with V_i being the intersection of the ith Cartesian voxel and the manually segmented myocardium in the 3D image, V_{tot} being the total volume of the myocardium, P_i being the number of identified microspheres in the ith voxel divided by V_i and P_{tot} being the total number of microspheres found in the myocardium divided by V_{tot}. $\bar{X}$ is the average number of particles found in each voxel and inversely proportional to the RD of the expected Poisson noise (Glenny *et al* 2000). Taking advantage of the arbitrary sampling of the data, the average RD at each voxel size is calculated at each voxel size and plotted double logarithmically as a function of the average volume of the intersection of each voxel with the segmented myocardium. Since the origin or corner of an aggregated voxel can be arbitrarily positioned on the CT image, the calculation of RD was repeated for eight different starting locations for an estimate of the standard deviation of RD. This type of origin resampling cannot be done with physically chopped up pieces of tissue and represents a distinct advantage of high-resolution imaging which leads to greater power in the statistical analysis.

Results

The phantom experiments clearly indicated that sufficient contrast is available in the CT images to detect individual microspheres. Figure 2 shows an optical micrograph of AgAuVIII microspheres (A), a maximum intensity projection (MIP) of the corresponding CT image perpendicular to the acrylic slide and an overlay of the micrograph with a MIP of the segmented CT image. By inspection, it can be seen that the optically identified microspheres correspond to bright spots on the microCT image. Bubbles seen in the optical image, however, do not show up on the microCT. It can also be seen that several aggregated microspheres on the optical image (A) show up as a single density on the microCT image. Figure 3 is a quantitative analysis of these data. Detection efficiency (TP fraction = TP/(TP+FN), where TP is the number of true positives and FN the number of false negatives) and false positive (FP) fraction = FP/(TP+FN), where FN is the number of false negatives, are plotted as a function of the detection threshold in figure 3. At a threshold level of 150 HU above the background, 80% of 381 microspheres were correctly detected and 4% were incorrectly detected. The fact that 20% of particles were not detected was primarily a consequence of the relatively high microsphere density in the phantom study, which meant that some microspheres were too close together to be resolved individually. Actually, only 3 of 381 microspheres seen in the optical images could not be associated with a high intensity island in the CT image. Using an approach to estimate particle number from the integrated intensity of connected voxels in the segmented image makes it possible to increase the detection efficiency to 96% but with a false positive fraction of 24%. In experimental studies with a somewhat lower particle density, detection efficiency is expected to be higher and false positive fraction lower than observed in the phantom study. For the AgVIII particles, 86% of 114 particles were correctly detected, and the false positive fraction was 4% at the same threshold level of 150 HU.

Figure 4 shows two images of microspheres in a rat heart after particle injection into the left atrium. Figure 4(A) is a maximum intensity projection (MIP) image through the whole heart showing all the microspheres. The microsphere density in this case was very high. Yet, most particles are clearly resolved. 35 694 particles were found in the myocardium.

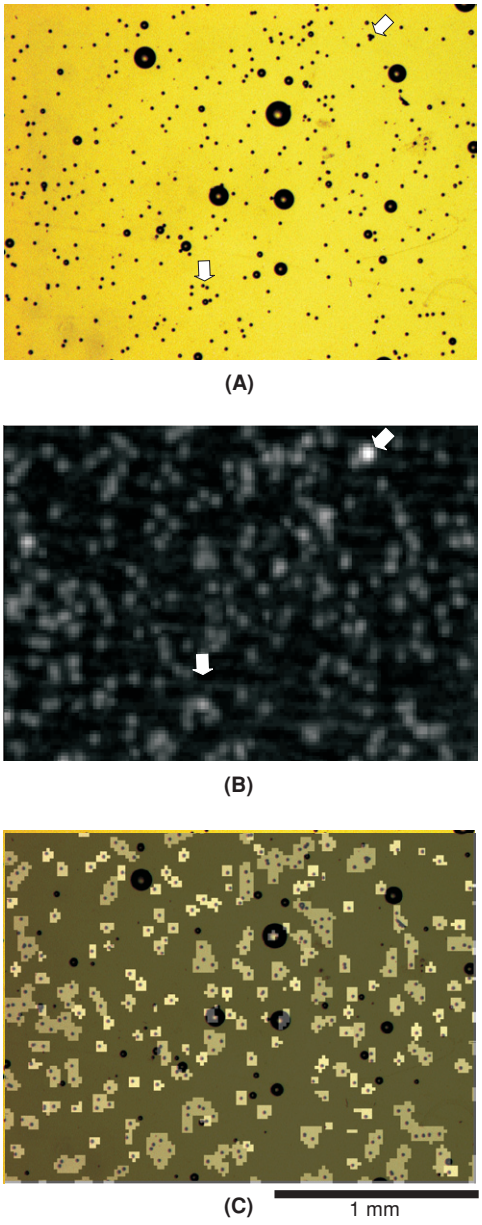

Figure 2. Optical image of a planar arrangement of microspheres (A), maximum intensity projection (MIP) of the corresponding CT image (B) and an overlay of the optical image with a MIP of the segmented and labelled CT image (C). The particle segmentation is done in the 3D images. Areas that appear connected in the MIP are therefore not necessarily connected in 3D. The large, dark spheres in the optical image are air bubbles, which do not appear in the MIP images. Examples of doublet microspheres that remain unresolved in the CT image are shown with arrows.

(This figure is in colour only in the electronic version)

Figure 4(B) shows the microspheres in a single slice with actual reconstructed densities (no MIP) of this 3D data set. This slice shows some of the anatomy and contains an outline

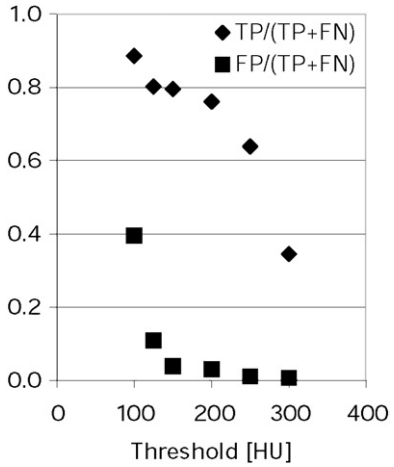

Figure 3. True positive fraction and false positive fractions in the detection of Ag/AuVIII microspheres for different CT threshold levels in Hounsfield units (HU) above the background. TP, FN and FP are the number of true positives, false negatives and false positives, respectively.

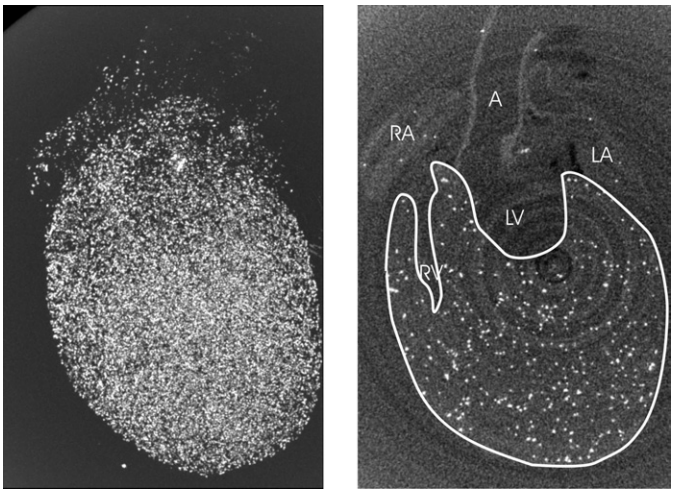

(A) (B)

Figure 4. Maximum intensity projection (MIP) of the three-dimensional CT image of a rat heart after microsphere injection into the left atrium (A) and an axial slice through the same data set with an outline of the myocardium and anatomical labels. (B) A, aorta; LA, left atrium; LV, left ventricle; RA, right atrium; RV, right ventricle. 35 694 particles were found in the segmented region. The field-of-view in both images is approximately 12 mm wide and the window and level setting lower than (B) to allow visualization of the soft tissues.

of the myocardium. Relative dispersion of perfusion for different voxel volumes is plotted in figure 5. The relative dispersion decreases from 0.354 ± 0.005 at 0.0597 mm^3 voxel volume to 0.12 ± 0.03 at 90 mm^3 voxel volume. Linear regression of the logarithmic data yields a slope of -0.14, which is comparable to previous observations in sheep, baboon and rabbit hearts (Bassingthwaighte *et al* 1989) made with radio-labelled microspheres.

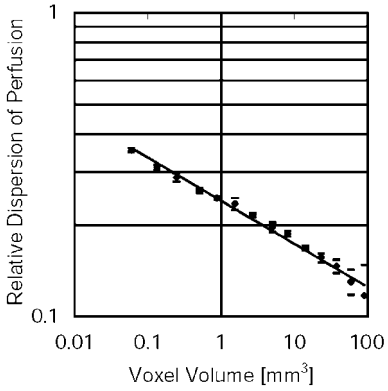

Figure 5. Relative dispersion of perfusion ± standard deviation is plotted as a function of voxel volume based on the microsphere deposition data displayed in figure 4. The slope of the linear regression line is −0.14 for the logarithmic data.

Discussion and conclusion

We have introduced silver/gold-coated microspheres for perfusion studies in this note and demonstrated the possibility of detecting these particles using a three-dimensional imaging technique. The microspheres could be manufactured at an appropriate diameter for perfusion studies of 17 μm and at a mass density of $\sim$2 g cm^{-3}. This mass density should be acceptable given that Prinzen and Bassingthwaighte state in their review of microsphere techniques (Prinzen and Bassingthwaighte 2000) that '. . . rheological properties of the microspheres are minimally affected by differences in their density' partially based on data by Reed and Wood (1970) in the density range from 0.2 to 3 g cm^{-3}.

The use of a non-destructive, high-resolution imaging technique to locate individual microspheres offers important advantages over other techniques that require dissection of the organ of interest. The resolution of the perfusion measurements is now only limited by the ability of the microspheres to represent the distribution of blood flow but no longer by the analysis technique. This is particularly relevant in the study of small animal organs. Multiple ROIs (regions of interest) with arbitrary boundaries can be selected. After the microCT imaging, further studies of the intact organ are possible. A major advantage is also convenience. The measurement result can be available within 24 h of the animal procedure and requires only a few hours of human experimental time. Glenny *et al* (2000) have also described a technique to obtain the locations of individual particles based on two-dimensional optical images of fluorescent particles in thin sections. Unlike three-dimensional imaging, the technique requires careful specimen preparation, slicing and registration of slices.

A major limitation of the microCT approach is that it is currently not possible to distinguish different kinds of microspheres. This limitation may be overcome in the future through use of coating materials with different K-edges in the x-ray absorption spectrum and scanning at varying x-ray energies.

Acknowledgments

This research is supported by the Canadian Institutes of Health Research and the National Cancer Institute of Canada. R Mark Henkelman is the recipient of a Canada Research Chair in Imaging.

References

Bassingthwaighte J B, King R B and Roger S A 1989 Fractal nature of regional myocardial blood flow heterogeneity *Circ. Res.* **65** 578–90

Feldkamp L A, Davis L C and Kress J W 1984 Practical cone-beam algorithm *J. Opt. Soc. Am.* A **1** 612–9

Glenny R W, Bernard S L and Robertson H T 2000 Pulmonary blood flow remains fractal down to the level of gas exchange *J. Appl. Physiol.* **89** 742–8

Heymann M A, Payne B D, Hoffman J I and Rudolph A M 1977 Blood flow measurements with radionuclide-labeled particles *Prog. Cardiovasc. Dis.* **20** 55–79

Kawallik P *et al* 1991 Measurement of regional myocardial blood flow in multiple colored microspheres *Circulation* **83** 974–82

Luchtel D C, Boykin J C, Bernard S L and Glenny R W 1998 Histological methods to determine blood flow distribution with fluorescent microspheres *Biotech. Histochem.* **73** 291–309

Marxen M, Thornton M M, Chiarot C B, Klement G, Koprivnikar J, Sled J G and Henkelman R M 2004 MicroCT scanner performance and considerations for vascular specimen imaging *Med. Phys.* **31** 305–13

Prinzen F W and Bassingthwaighte J B 2000 Blood flow distributions by microsphere deposition methods *Cardiovasc. Res.* **45** 13–21

Reed J H Jr and and Wood E H 1970 Effect of body position on vertical distribution of pulmonary blood flow *J. Appl. Physiol.* **28** 303–11

Wieland W, Wouters P F, Van Aken H and and Flameng W 1993 Measurement of organ blood flow using coloured microspheres: a first time-saving improvement using automated spectrophotometry *Computers in Cardiology* (Los Alamitos, CA: IEEE Society Press) pp 691–4